El Niño Southern Oscillation during the Medieval Climate Anomaly

Gerald T. Rustic[1, 2], Athanasios Koutavas[1,2,3], Braddock K. Linsley[3]

[1]Department of Engineering, Science and Physics, College of Staten Island, Staten Island, NY; [2]Doctoral Program in Earth and Environmental Science, CUNY Graduate Center, New York, NY; [3]Lamont-Doherty Earth Observatory, Columbia University, Palisades, NY

THE GRADUATE CENTER
CITY UNIVERSITY OF NEW YORK

THE CITY UNIVERSITY OF NEW YORK
College of Staten Island

Abstract: The dynamic response of the El Niño Southern Oscillation (ENSO) to varying solar and volcanic forcing is thought to be an important influence on climate during the Medieval Climate Anomaly (MCA), but proxy evidence of ENSO variability during the MCA is sparse. Here we analyze $\delta^{18}O$ of individual mixed-layer dwelling foraminifera *Globigerinoides ruber* from a high-resolution (>10cm/ky) multi-core (MC42) from the Eastern Tropical Pacific (Figure 1) to test the hypothesis that ENSO variability was different in the MCA compared to the 20th Century. We found that $\delta^{18}O$ from instrumental-era samples captured the variability and full range of oceanographic conditions predicted by $\delta^{18}O$ calculated from oceanographic reanalysis data, including peak El Niño and La Niña conditions (Figure 3) and that multi-decadal scale variability in calculated $\delta^{18}O$ is reflected in foraminifera $\delta^{18}O$ from instrumental era populations (Figure 2). We also found that $\delta^{18}O$ from individual foraminifera from ≈1100-1300CE display variability reductions from 27% to 33% compared to late 20th Century values, as well as reduced range and fewer $\delta^{18}O$ outliers (Figure 4), suggesting weaker ENSO activity during the MCA. This reduction is consistent with existing paleoclimate reconstructions and the modeled response of the tropical Pacific to increased solar forcing during the MCA.

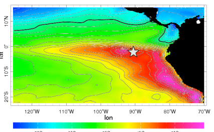

Figure 1. Study location (star) showing the average March-September SST difference 1890-2008. SST variability at this location is strongly influenced by the seasonal cycle and by ENSO (Map from IRIDL/IRIS)

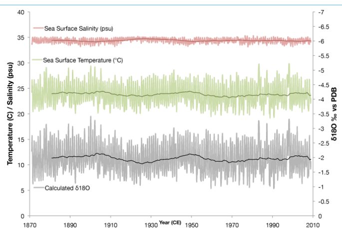

Figure 2. Sea Surface Temperature (SST), Sea Surface Salinity (SSS) and calculated $\delta^{18}O$ from Simple Ocean Data Assimilation (SODA) 2.2.4 (Carton and Giese 2012) 1871-2008. $\delta^{18}O$ values for each month were calculated based on SODA SST and SSS values using the high-light equation from Bemis (1998) and seawater/salinity equation from Fairbanks (1982). The 10-year moving average is plotted as darker lines on each time series. Note the reduction in $\delta^{18}O$ in the early 20th Century. This period also featured lower $\delta^{18}O$ variability (see Figure 3).

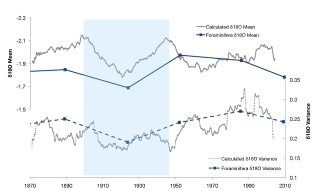

Figure 3. Variance and mean for calculated δ18O and foraminifera δ18O, 1871-2008. Calculated $\delta^{18}O$ values (gray lines) are 10-year running mean and 10-year running variance smoothed with a 13-point binomial filter. Boxes on foraminifera $\delta^{18}O$ plots indicate the modeled date at top of each interval. Both mean and variance of calculated and foraminifera $\delta^{18}O$ show coincident decreases in the early 20th Century (shaded area).

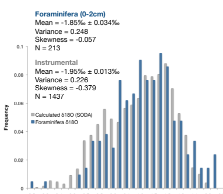

Figure 4. Distribution of calculated $\delta^{18}O$ and foraminifera $\delta^{18}O$, 1890-2008. Calculated $\delta^{18}O$ spans the age range for the top 2cm of core MC42C. The mean (t-test $p<0.05$) and variance of each population is statistically identical ($F >>0.05$).

Materials and methods

KNR195-5 MC42 was collected in 2009 from the Galapagos Islands (01° 15.18'S, 89° 41.13'W, 615m depth). Section MC42C was sampled at ~0.5cm intervals (~40 years). ^{14}C dates from core MC42C and MC42E indicate that the core-top sediments are modern and sedimentation rates are 10-14cm/ky based on a mass-dependent linear interpolation age model. Individual *G. ruber* were picked from the 300-355um size fractions. Analysis of samples presented here were performed at the Lamont Doherty Earth Observatory with an analytical precision of <0.11‰. Instrumental temperature and salinity data for calculating predicted $\delta^{18}O$ are from SODA (Simple Ocean Data Assimilation – SODA) version 2.2.4 (Carton and Giese, 2012) for 1871-2008 for the 0.5°x0.5° grid box around the study site. Predicted $\delta^{18}O$ was calculated with the high-light equation of Bemis et al. (1998) and the seawater/salinity equation of Fairbanks et al. (1982).

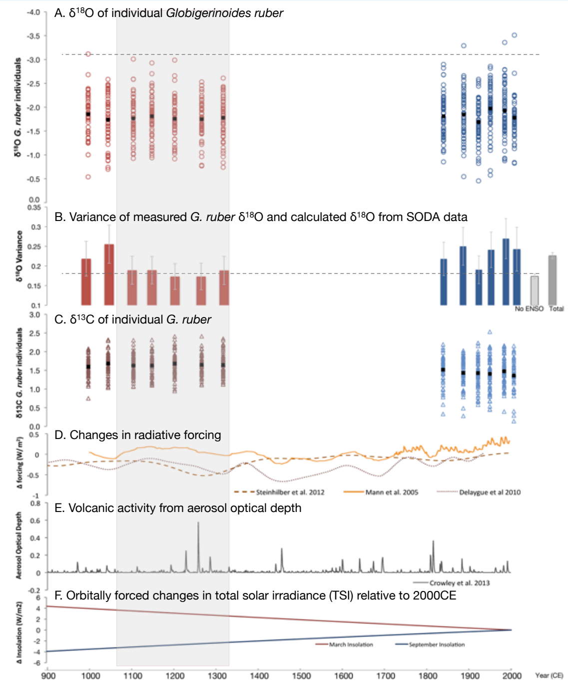

Figure 5. Foraminifera $\delta^{18}O$ and $\delta^{13}C$ with climate forcings. Shaded area is the peak MCA, ≈1100-1300CE.

***A) G. ruber* $\delta^{18}O$ distributions.** The range and variance of core-top samples (blue) is greater than the range and variance of MCA intervals (red). Each circle is measured $\delta^{18}O$ from an individual *G. ruber*. Dotted line indicates $\delta^{18}O$ values seen only during El Niño conditions in the modern instrumental record.

B) $\delta^{18}O$ Variance for each sample interval. The gray bar (far right) is total variance for the calculated 20th Century $\delta^{18}O$ values. The No ENSO variance (light gray bar) is the variance of the seasonal cycle from calculated $\delta^{18}O$ monthly averages, effectively removing the ENSO component of variability. Removing the ENSO component reduces total variance of calculated $\delta^{18}O$ by 23%. The average variance reduction of foraminifera $\delta^{18}O$ during the peak MCA intervals (≈1100-1300) is 30% compared to 20th Century foraminifera $\delta^{18}O$ variance. Through the entire MCA (999-1300) variance is reduced on average 24%.

***C) G. ruber* $\delta^{13}C$ distributions.** MCA era samples display significantly increased mean $\delta^{13}C$ values (student's t-test $p<0.05$) and significant reductions in variance ($f > 0.05$). Average MCA $\delta^{13}C$ variance (0.087) is reduced by 50% compared to 20th Century $\delta^{13}C$ variance (0.181). Total $\delta^{13}C$ range is also reduced in the MCA, and no $\delta^{13}C$ depleted outliers are observed. As $\delta^{13}C$ is inversely related to dissolved nutrient concentrations (Marchitto 2013), reduced variance and range of $\delta^{13}C$ values may indicate a reduction of upwelling consistent with less active ENSO.

D) Change in Radiative Forcing 30-year smoothed modeled tropical solar forcing (solid line, Mann et al. 2005); Antarctic ice ^{10}Be-based TSI (dotted line, Delaygue et al. 2010) and globally-averaged ice-based ^{10}Be and tree-ring based ^{14}C (dashed line, Steinhilber et al. 2010) TSI reconstructions with 13-point binomial filter applied. Values are relative to the last published date in each data set (2000CE, 1986CE and 1982CE, respectively).

E) Volcanic forcing, showing global aerosol optical depth for the past 1100 years (Crowley et al. 2013).

F) March and September insolation changes at the equator due to orbital forcing, relative to 2000CE (Laskar et al. 2004).

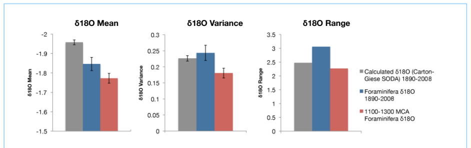

Figure 6. Comparison of calculated $\delta^{18}O$ from SODA 1890-2008 (gray), foraminifera $\delta^{18}O$ 1890-2008 (blue) , and peak MCA foraminifera $\delta^{18}O$ (≈1100-1300). Means are statistically identical ($p<0.05$, student's t-test). The variance (middle figure) for calculated $\delta^{18}O$ (0.248) and foraminifera $\delta^{18}O$ (0.261) is statistically identical. The peak MCA foraminifera $\delta^{18}O$ variance (0.181) shows significant $\delta^{18}O$ reduction of 26% from 1890-2008 foraminifera $\delta^{18}O$ variance. The range of the peak MCA $\delta^{18}O$ values is smaller than both calculated and foraminifera $\delta^{18}O$ from 1890-2008. The 1890-2008 values contain several negative $\delta^{18}O$ outliers, while the MCA samples do not (Grubb's test for outliers; see Figure 5A).

Conclusions

1. **Do core-top distributions of individual foraminifera $\delta^{18}O$ reflect modern oceanographic conditions at the sample site?**
   - **YES** – we find that $\delta^{18}O$ distribution of modern *G. ruber* is statistically identical to calculated values from reanalysis data at various time intervals in the instrumental era (Figure 3).
2. **Is there evidence for multi-decadal resolution?**
   - **YES** – *G. ruber* $\delta^{18}O$ data appear to capture a distinct period of cooler SSTs and decreased ENSO variance in the early 20th Century.
3. **Is there evidence for changes in the $\delta^{18}O$ characteristics between modern and MCA samples?**
   - **YES** – the $\delta^{18}O$ standard deviation and variance are significantly reduced in samples from ≈1100-1300 as compared to 20th Century intervals (Figure 5).
4. **Is there evidence of reduced ENSO activity during the MCA?**
   - **YES** – foraminifera $\delta^{18}O$ from peak MCA intervals display reduced variance, smaller range and fewer statistical outliers compared to late 19th-20th Century foraminifera populations. This reduction of $\delta^{18}O$ variability is on the scale of removal of ENSO from late 19th-20th Century $\delta^{18}O$ values. $\delta^{13}C$ variance reduction in the MCA may indicate reduced upwelling. It is likely the changes in total oceanographic variability are due to reductions in both seasonality and ENSO variability during the MCA.

References

Bemis, B. E., Spero, H. J., Bijma, J. & Lea, D. W. Reevaluation of the oxygen isotopic composition of planktonic foraminifera: Experimental results and revised paleotemperature equations. *Paleoceanography* **13,** 150–160 (1998).

Carton, J.A. and Giese, B.S. *CARTON-GIESE SODA SODA 2.2.4, 1871-2008 Assimilation Run: Oceanic and air-sea interface data from the UMD Simple Ocean Data Assimilation Reanalysis.* (2012).

Clement, A. C., Seager, R., Cane, M. A. & Zebiak, S. E. An ocean dynamical thermostat. *Journal of Climate* **9,** 2190–2196 (1996).

Crowley, T. J. & Unterman, M. B. Technical details concerning development of a 1200 yr proxy index for global volcanism. *Earth System Science Data* **5,** 187–197 (2013).

Delaygue, G. and E. Bard. *Antarctic Last Millennium 10Be Stack and Solar Irradiance Reconstruction.* (IGBP PAGES/World Data Center for Paleoclimatology Data Contribution Series # 2010-035. NOAA/NCDC Paleoclimatology Program, Boulder CO, USA., 2010).

Fairbanks, R. G., Sverdlove, M., Free, R., Wiebe, P. H. & Bé, A. W. H. Vertical distribution and isotopic fractionation of living planktonic foraminifera from the Panama Basin. *Nature* **298,** 841–844 (1982).

Gao, C., et al. *1500 Year Ice Core-based Stratospheric Volcanic Sulfate Data.* (IGBP PAGES/World Data Center for Paleoclimatology Data Contribution Series # 2009-098. NOAA/NCDC Paleoclimatology Program, Boulder CO, USA., 2009).

Hansen, J. Efficacy of climate forcings. *Journal of Geophysical Research* **110,** (2005).

Koutavas, A. & Joanides, S. El Niño–Southern Oscillation extrema in the Holocene and Last Glacial Maximum. *Paleoceanography* **27,** (2012).

Laskar, J. *et al.* A long-term numerical solution for the insolation quantities of the Earth. *Astronomy and Astrophysics* **428,** 261–285 (2004).

Mann, M.E., et al. *Volcanic and Solar Forcing of the Tropical Pacific over the Past 1000 Years*. (IGBP PAGES/World Data Center for Paleoclimatology Data Contribution Series # 2005-035. NOAA/NGDC Paleoclimatology Program, Boulder CO, USA., 2005).

Marchitto T.M. (2013) Nutrient Proxies. In: Elias S.A. (ed.) The Encyclopedia of Quaternary Science, vol. 2, pp. 899-906. Amsterdam: Elsevier.

Steinhilber, F., et al. *9400 Year Cosmogenic Isotope Data and Solar Activity Reconstruction.* (IGBP PAGES/World Data Center for Paleoclimatology Data Contribution Series # 2012-040. NOAA/NCDC Paleoclimatology Program, Boulder CO, USA., 2012).